Hierarchical models of rigidity percolation

J. Barré
Laboratoire J. A. Dieudonné, UMR CNRS 6621, Université de Nice–Sophia-Antipolis, Parc Valrose, F-06108 Nice Cedex 2, France
(Received 16 July 2009; revised manuscript received 21 October 2009; published 8 December 2009)

We introduce models of generic rigidity percolation in two dimensions on hierarchical networks and solve them exactly by means of a renormalization transformation. We then study how the possibility for the network to self organize in order to avoid stressed bonds may change the phase diagram. In contrast to what happens on random graphs and in some recent numerical studies at zero temperature, we do not find a true intermediate phase separating the usual rigid and floppy ones.

DOI: 10.1103/PhysRevE.80.061108 PACS number(s): 64.60.ah, 64.60.ae, 05.10.Cc

I. INTRODUCTION

Consider a structure made of sites connected by links. Each link imposes a constraint, by prescribing the distance between the two sites it connects: if the actual distance between the two sites is different from the prescription, there is an associated energy cost. Rigidity theory deals with properties associated with the structure's topology, which do not depend on the physical nature of the constraints nor on the precise form of the energy cost. Typical questions asked by rigidity theory are: how many degrees of freedom are left in the system? Is there a macroscopic cluster of sites rigidly connected one with the others? By contrast, questions related to the elastic properties of the structure do depend on the specification of the constraints. When the number of links in the structure is increased, the phenomenology is as follows. For a small enough number of links that is a small mean connectivity of the structure, there are many more degrees of freedom than constraints; there is no macroscopic rigid cluster, and many degrees of freedom are left in the system: the system is said to be floppy. At large mean connectivity, there are many more constraints than degrees of freedom; there is a macroscopic rigid cluster, and many constraints cannot be satisfied: the system is said to be stressed rigid. In between these two phases takes place the rigidity percolation transition.

Despite its clearly mechanical origin, the problem of rigidity percolation has also attracted attention in the last 30 years because of its applications in understanding the properties of network forming glasses, such as GeSe or GeAsSe alloys [1,2]. In this case, the atomic bonds may be considered as constraints. However, contrary to standard rigidity percolation as presented in the first paragraph, angles between adjacent bonds also need to be considered as constraints, in addition to bond lengths. In the following, we will concentrate on central force rigidity (that is when only bond lengths are considered as constraints) in two dimensions. Beyond the applications to glasses, models of cross linking stiff fibers forming random networks were shown to fall in the same universality class as central force two-dimensional (2D) rigidity [3]; this type of system has been used to model network forming proteins [4].

A decisive theoretical progress was made in the 1990s for *generic* [37] 2D rigidity, with the introduction of combinatorial algorithms [6,7] based on Laman's theorem [8]. These algorithms allow for the study of much larger samples than before as well as more precise estimates around the critical point [9]. In particular, for rigidity percolation on regular lattices, the scenario of a second-order phase transition in a different universality class than ordinary percolation seems favored by the numerics although there has been some debate on the subject [10].

From the analytical point of view however, progresses have been slow. A field theoretical attempt by Obukhov [11] predicts a first-order phase transition in 2D, which, when compared with the numerics, seems to be a nongeneric feature. Some insight came from rigidity models exactly solved on trees and various types of random graphs, with locally treelike topology [10,12–15]. However, in these types of models, the rigidity percolation transition is also usually first order. This casts doubt on their usefulness to understand generic 2D rigidity. There has been also earlier attempts to study rigidity percolation through position space renormalization group [16,17]; based on small renormalization cells, the associated predictions for the critical exponents are unprecise. To this date, we are not aware of any precise analytical prediction for the critical exponents of 2D generic rigidity percolation.

A few years ago, Thorpe *et al.* opened a research direction by introducing the notion of network self-organization in rigidity percolation models [18]. This is a natural idea in the context of network glasses modeling: constraints that are not satisfied create stress and bear an energy cost; the network should then self-organize, i.e., tend to modify its structure, in order to minimize this energy cost. In [18], numerical simulations allowing self-organization point to the existence of a third phase in between the usual floppy and rigid ones. As a function of the mean connectivity, the phase diagram would then show two phase transitions instead of one. Around the same time, several experiments on network glasses drew a picture compatible with this predicted phenomenology [19–21]. A problem of the original simulations of [18] was their strongly out of equilibrium character; some theoretical studies improved on this, and confirmed the "three phases" picture [22,23]. In [24,25], a class of self-organizing rigidity percolation models is exactly solved and shows three phases separated by two true thermodynamic phase transitions. However, these exactly solvable models are based on random networks, which have a locally tree like topology, without small loops. This strongly influences the critical properties of the rigidity transition; in particular, as already mentioned

above, rigidity percolation is continuous for a regular 2D triangular network, and it is first order in random networks. The simulations of Refs. [26,27], performed at zero temperature on a triangular lattice, seem to confirm the phenomenology suggested by the locally treelike random networks studies and show that the entire intermediate phase has a critical nature. Sartbaeva *et al.* in [28] discuss the influence of local structures on the existence and width of the intermediate phase in more realistic network glasses models. Despite these works, the question of whether self-organized rigidity percolation on two dimensional networks at finite temperature displays a true "intermediate phase" is still open. We conclude this paragraph by mentioning recent reviews on the subject [29,30].

The goal of this paper is twofold. First, we introduce a class of solvable models of 2D rigidity on hierarchical lattices. These lattices, in contrast with random graphs are not locally treelike and possess many small loops. We may then expect for these lattices a phenomenology closer to generic 2D rigidity than random graphs. It is known that models defined on hierarchical lattices may be exactly solvable using renormalization transformations [31–33]; we will use the same ideas in the context of rigidity percolation. Second, in the spirit of [24] for random networks, we add to the hierarchical networks the possibility of self-organization. This provides a class of exactly solvable models, genuinely different from the random graphs of [24,25], where it is possible to investigate the existence of an intermediate phase.

The paper is organized as follows. In Sec. II, we summarize the combinatorial approach to 2D rigidity, which will be necessary in the following. After introducing, in Sec. III, the class of hierarchical lattices we will be interested in, we solve our model and study its critical properties in Sec. IV. We then introduce the possibility of self-organization for the hierarchical networks and solve the associated model in Sec. V; we discuss the implications on the existence of an intermediate phase between the usual floppy and stressed rigid ones. Section VI is devoted to discussion and perspectives.

II. GENERIC 2D RIGIDITY

An intuitive approach to rigidity percolation, apparently due to Maxwell, consists in counting degrees of freedom and constraints. In two dimensions, each site has two degrees of freedom; each link brings one constraint. In the end, a certain number of degrees of freedom are left. They correspond to unconstrained motions of the sites, and are usually called "floppy modes." If one thinks of each link as a spring, with a given rest length, floppy modes are motions of the sites that do not change any spring length and thus do not cost any energy. Any network embedded in two dimensions necessarily has at least three floppy modes, corresponding to the two global translations and the global rotation in the plane. The network or a subgraph of the network is said to be rigid if it has no internal degree of freedom besides these three. In a first approximation, a network with N sites and M links should have

$$N_{flop} = \max(3, 2N - M) \tag{1}$$

degrees of freedom left, and be rigid if $2N-M \leq 3$. This simple computation is obviously wrong in general, as shown on Fig. 1. The reason is that when a new bond is added, it may be "redundant:" then the constraint associated with this new bond cannot be satisfied and its addition does not remove any degree of freedom. The exact formula giving the number of floppy modes of a network is

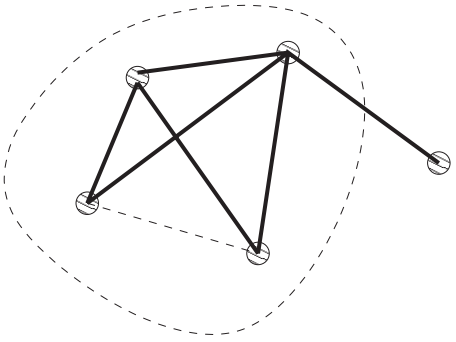

FIG. 1. An example of a graph with $N=5$ sites. Before the addition of the dashed bond, there are $M=6$ bonds, none of which is redundant. The number of floppy modes is 4: two global translations, one global rotation, and the additional rotation of the one-coordinated site. The dashed bond is redundant: the subgraph isolated by the dashed curve has $N_{sub}=4$ sites and $M_{sub}=6>2N_{sub}-3$ bonds. The whole graph with the dashed bond also has four floppy modes, in agreement with Eq. (2).

$$N_{flop} = 2N - M + N_{red}, \tag{2}$$

where N_{red} is the number of redundant bonds. The problem is then reduced to the estimation of N_{red}. The simplest form of Maxwell counting given by Eq. (1) assumes that new bonds added in the network first exhaust the degrees of freedom available before starting to become redundant. It is not correct, but it turns out that a generalization of this idea is actually exact [8]. It may be formulated as follows. Consider a graph, and add a new bond to it. It is redundant if and only if there exists a subgraph with N_{sub} sites and M_{sub} bonds, containing this new bond, such that $2N_{sub}-M_{sub}<3$. This combinatorial formulation is at the root of the "pebble game," a powerful algorithm to analyze rigidity percolation on two dimensional networks [6,7].

III. HIERARCHICAL LATTICES

We will consider the following type of hierarchical graphs. We start from two sites, connected by one bond. The graph is then constructed iteratively; at each step, all bonds are replaced by a given elementary cell. Four examples of elementary cells, corresponding to four examples of hierarchical graphs, are given on Fig. 2. In each case, it is easy to obtain a recursion relation for the number of sites N_t and bonds B_t of the graphs after t iterations. We obtain, respectively, for the four graphs of Fig. 2

$$B_{t+1}^{(1)} = 9B_t^{(1)}, \quad N_{t+1}^{(1)} = N_t^{(1)} + 3B_t^{(1)}, \tag{3}$$

$$B_{t+1}^{(2)} = 5B_t^{(2)}, \quad N_{t+1}^{(2)} = N_t^{(2)} + 2B_t^{(2)}, \tag{4}$$

$$B_{t+1}^{(3)} = 12B_t^{(3)}, \quad N_{t+1}^{(3)} = N_t^{(3)} + 5B_t^{(3)}, \tag{5}$$

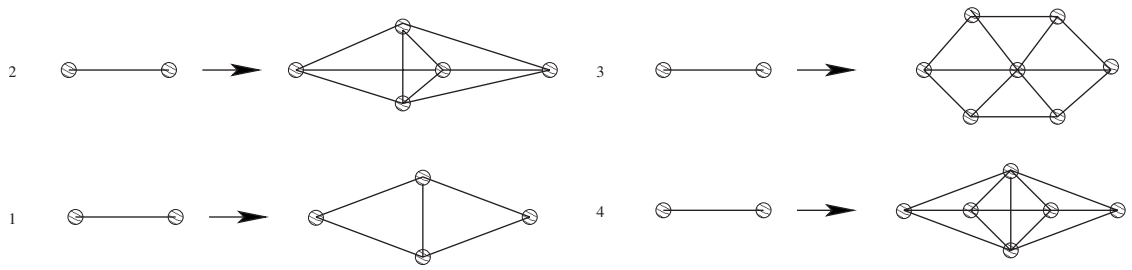

FIG. 2. Four examples of hierarchical graphs. On the left, the graphs at step $t=0$, with two sites and one bond; on the right, the graphs at $t=1$. We call the $t=1$ graph the "elementary cell." (1) is an elementary cell with five sites and nine bonds. This is the hierarchical graph we will mostly consider in the following. (2), (3) and (4) are elementary cells with, respectively, four sites and five bonds, seven sites and 12 bonds, and six sites and 12 bonds. At step t, each bond of step $t-1$ is replaced by a subgraph identical to the $t=1$ graph.

$$B_{t+1}^{(4)} = 12B_t^{(4)}, \quad N_{t+1}^{(4)} = N_t^{(4)} + 4B_t^{(4)}. \tag{6}$$

Solving these recursion relations yields:

$$B_t^{(1)} = 9^t, \quad N_t^{(1)} = \frac{3 \times 9^t + 13}{8}, \tag{7}$$

$$B_t^{(2)} = 5^t, \quad N_t^{(2)} = \frac{5^t + 3}{2}, \tag{8}$$

$$B_t^{(3)} = 12^t, \quad N_t^{(3)} = \frac{5 \times 12^t + 17}{11}, \tag{9}$$

$$B_t^{(4)} = 12^t, \quad N_t^{(4)} = \frac{4 \times 12^t + 18}{11}. \tag{10}$$

To model the rigidity percolation phenomenon, we now assume that each bond is effectively present in the graph with probability p; thus, the number of occupied bonds is, for large graphs, $M_t \simeq pB_t$. The Maxwell counting procedure yields an estimate of the threshold for rigidity percolation: the approximate critical probability p_{Max} corresponds to a ratio between bonds and sites $M_t/N_t=2$. For graph on Fig. 2(2), we find $p_{\mathrm{Max}}^{(2)}=1$; any $p<1$ should then render this graph floppy, and there is no true rigidity percolation. We thus dismiss this example in the following. For the graphs on Figs. 2(1), 2(3), and 2(4), we find, respectively, $p_{\mathrm{Max}}^{(1)}=3/4$, $p_{\mathrm{Max}}^{(3)}=10/11$, and $p_{\mathrm{Max}}^{(4)}=8/11$. All three graphs should then present a rigidity transition at $p<1$. We will mainly concentrate in the following on graph (1) for the sake of simplicity.

IV. SOLUTION OF THE HIERARCHICAL MODELS

The goal is to compute a recursion relation relating $N_t^{red}(p)$, the number of redundant bonds of a graph iterated t times, with a bond occupation probability p, and $N_{t-1}^{red}(p')$, the number of redundant bonds of a graph iterated $t-1$ times, with a bond occupation probability p'. This will be possible because of the peculiar structure of the network [32].

The procedure is somewhat reciprocal to the construction of the hierarchical network. Consider a graph iterated t times, with a bond probability p. Consider two sites A and B separated by one elementary cell, see Fig. 3. If they are rigidly connected through this cell, we replace the whole cell by a single bond. If they are not, we delete the whole cell. Repeating this procedure for all elementary cells, we construct a new graph, iterated $t-1$ times, with a bond occupation probability $p'=\varphi(p)$. The function $\varphi(p)$ is constructed by counting all configurations leading to a rigid connection between A and B. This process is detailed on Table I, for the graph on Fig. 2(1).

Collecting the different contributions, we obtain

$$\varphi(p) = p^9 + 9p^8q + 30p^7q^2 + 12p^6q^3 + 3p^5q^4, \tag{11}$$

where $q=1-p$. We assume that the number of redundant bonds is an extensive quantity; neglecting subdominant contributions and probabilistic fluctuations, we then write

$$N_t^{red}(p) = N_t r(p), \tag{12}$$

and our goal is to compute $r(p)$. Analyzing one renormalization step, we write

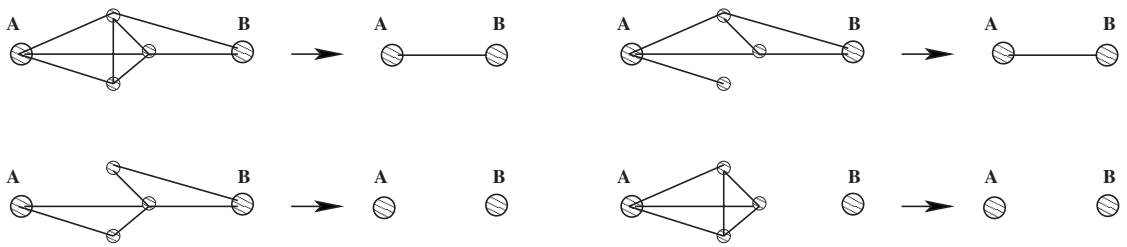

FIG. 3. Renormalization of an elementary cell, and counting of redundant bonds. Top left: sites A and B are rigidly connected so that the elementary cell is renormalized into a bond; there is one redundant bond. Top right: sites A and B are rigidly connected, no redundant bond. Bottom left: sites A and B are not rigidly connected, no redundant bond. Bottom right: sites A and B are not rigidly connected, one redundant bond.

TABLE I. Enumeration of all types of possible configurations for an elementary cell of the graph on Fig. 2(1). There are for instance 12 configurations with six bonds, providing a rigid connection across the cell and without redundant bond. Some examples are given on Fig. 3.

No. bonds	Rigid connection	No. redundant bonds	No. configurations
9	Yes	2	1
8	Yes	1	9
7	Yes	0	30
7	No	1	6
6	Yes	0	12
6	No	0	70
6	No	1	2
5	Yes	0	3
5	No	0	123
4	No	0	126
3	No	0	84
2	No	0	36
1	No	0	9
0	No	0	1

$$N_t^{red}(p) = N_{t-1}^{red}[\varphi(p)] + N'_{red}(t,p), \tag{13}$$

where $N'_{red}(t,p)$ represents all the redundant bonds that where suppressed in the renormalization process. This formula needs some justification. Consider the empty (without bonds) graph at step t and add the bonds one by one, checking each time if the newly added bond is redundant or not; this is actually the numerical strategy implemented in the pebble game algorithm. If the added bond is redundant, it is discarded. Thus, during the process, the constructed graph has at most one redundant bond. If an added bond is redundant, it is possible to find a subgraph S, containing this new bond, with N_{sub} sites and $M_{sub}=2N_{sub}-2$ bonds. We choose S as small as possible. There are now two possibilities. Either S is included in one elementary cell; in this case the redundant bond is included in the $N'_{red}(t,p)$ contribution. Or S is not included in an elementary cell. It is easy to see that no floppy elementary cell can be included in S so that the newly added bond necessarily "rigidifies" the elementary cell it belongs to. In addition, if S contains a bond included in one elementary cells, S contains both sites which are end points of the cell, and the cell is rigid. S, which is included in the graph at step t will then be renormalized in a natural way in a subgraph of the graph at step $t-1$. The redundant constraint is thus included in the $N_{t-1}^{red}[\varphi(p)]$ contribution to Eq. (13). It is worth mentioning that both the hierarchical nature of the graph and the convenient combinatorial description of 2D rigidity outlined in Sec. II are necessary for this step. In particular, it is not clear how to construct exactly solvable hierarchical models of three-dimensional (3D) rigidity.

For a given bond probability p, we want to compute $r_0(p)$, the mean number of redundant bonds inside one elementary cell. We use Table I to enumerate all possibilities, and we obtain the following expression for $r_0(p)$:

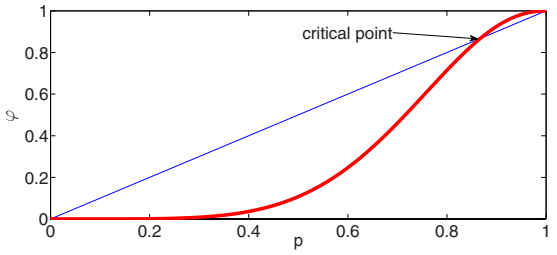

FIG. 4. (Color online) The red curve $y=\varphi(p)$ (thick line), together with the blue $y=p$ straight line (thin line). The critical point defined by $\varphi(p^*)=p^*$ is indicated by an arrow.

$$r_0(p) = 2p^9 + 9p^8q + 6p^7q^2 + 2p^6q^3. \tag{14}$$

In one renormalization step, a large number of elementary cells B_{t-1} is renormalized. Thus $N'_{red}(t,p) \simeq B_{t-1}r_0(p)$. Finally, the recursion relation reads as

$$N_t r(p) = N_{t-1} r[\varphi(p)] + B_{t-1} r_0(p). \tag{15}$$

Using the relations $B_t=B^t$ and $B_t/N_t=x_0$, and simplifying by N_t, this yields

$$r(p) = \frac{1}{B} r[\varphi(p)] + \tilde{r}_0(p), \tag{16}$$

with $\tilde{r}_0(p)=x_0 r_0(p)/B$. For our main example, represented on Fig. 3, $B=9$ and $x_0=8/3$.

From Eq. (2), we see that for given numbers of sites and bonds, the number of floppy modes is linearly related to the number of redundant bonds. Since it has been noticed [10] that the number of floppy modes plays the role of a "free energy" in rigidity percolation models, we remark that the computation of $r(p)$ is analogous to the free-energy computation of Ref. [33] for spin models on hierarchical lattices.

The function φ is plotted on Fig. 4. It has three fixed points; $p=0$ and $p=1$ are stable and correspond to the floppy and rigid phases, respectively. $p=p^* \simeq 0.867$ is unstable and is the critical point. We note $\varphi^{(k)}$ the kth iterate of φ. Then for all $p<p^*$ (respectively, $p>p^*$), $\varphi^{(n)}(p)$ tends to 0 (respectively, 1). The quantity $a=d\varphi/dp(p=p^*) \simeq 1.97$ will play an important role. We note that if we had used the hierarchical network on Fig. 2(2), we would have obtained a function φ with only two fixed points: $p=0$ (stable) and $p=1$ (unstable). Thus, in this case, any $p<1$ yields a floppy network at large scales. A similar analysis for the graphs on Figs. 2(3) and 2(4) yields, respectively, $p^*=0.975$ and $p^*=0.853$ for the critical densities and $a=1.86$ and $a=2.07$ for the φ derivative at criticality. We note that in all three cases, we find $p^* > p_{\mathrm{Max}}$.

Iterating n times Eq. (16), one obtains

$$r(p) = \frac{1}{B^n} r[\varphi^{(n)}(p)] + \frac{1}{B^{n-1}} \tilde{r}_0[\varphi^{(n-1)}(p)] + \cdots + \frac{1}{B} \tilde{r}_0[\varphi(p)] + \tilde{r}_0(p). \quad (17)$$

As $B>1$ and $\tilde{r}_0$ is bounded, r may then be expressed as an infinite series:

$$r(p) = \sum_{k=0}^{\infty} \frac{1}{B^k} \tilde{r}_0[\varphi^{(k)}(p)]. \quad (18)$$

As the k times iterated function $\varphi^{(k)}(p)$ tends pointwise to 0 when $p<p^*$ and to 1 when $p>p^*$, the above series is infinitely differentiable, except when $p=p^*$, the unstable fixed point of φ. Looking for a power-law behavior of r close to p^*

$$r(p) = \text{const } |p - p^*|^{\tau} + \text{regular part}, \quad (19)$$

one finds $\tau = \ln B / \ln a$. For our main example, we find $\tau = 3.24$; this corresponds to a critical exponent $\alpha = -1.24$, where we have used the standard notation for the critical exponent associated with the free-energy singularity. This means that the derivatives of $r(p)$ are all continuous up to third order, while the fourth derivative is discontinuous. This does not compare well to the numerical results on triangular networks [9], which find $\alpha \simeq -0.48$. Networks on Figs. 2(3) and 2(4) yield, respectively, $\tau = 4.01$ and $\tau = 3.41$, which corresponds to $\alpha = -2.01$ and $\alpha = -1.41$. Thus, there are important fluctuations in the value of the critical exponent between two different hierarchical networks. We note however that the tendency to a very weak rigidity percolation transition on these hierarchical networks seems to be general. A natural idea to improve the agreement between these analytical results on hierarchical networks and the numerics on triangular lattices would be to consider larger renormalization cells. The previous remarks cast doubt on this strategy. Another interesting extension would be to study other critical properties, such as the size of the largest rigid cluster or the largest stressed cluster.

V. ADAPTIVE NETWORKS

A. Introduction of an energy

We consider now the possibility for the network to modify its structure, in order to avoid stress. This step was first taken in [18], in an attempt to better model network glasses; in this context, it is natural to assume that the connectivity structure of the network may adapt itself to a certain extent to avoid stressed bonds. Following [24], we introduce an energy cost for each constraint which is not satisfied; at any finite temperature, this cost competes with the entropic cost of reorganizing the network. In this setting, standard rigidity percolation, as studied up to now, corresponds to the infinite temperature limit, where the energy cost is negligible.

We have to define an energy for any configuration of the network. The simplest choice is to count the number of redundant bonds and to attribute the same amount of energy to each of them [24,25].

We consider a network where a proportion x of the bonds is present. The partition function for our model on a hierarchical network iterated t times reads as

$$Z_t(x,\beta) = \sum_{\{l_j\}, \Sigma l_j = x B_t} e^{-\beta N_{red}(\{l_j\})}, \quad (20)$$

where we note $l_j=1$ if bond j is present $l_j=0$ otherwise; $\Sigma_{\{l_j\}}$ is the sum over all possible configurations of the network. Here, it is restricted to the configurations with the prescribed fraction of occupied bonds, x.

To proceed, it is useful to relax the constraint on the number of bonds. We introduce a "grand canonical" statistical ensemble, whose partition sum reads as

$$\Omega_t(p,\beta) = \sum_{\{l_j\}} p^{\Sigma l_j} q^{B_t - \Sigma l_j} e^{-\beta N_{red}(\{l_j\})}, \quad (21)$$

where p is the *a priori* probability that a bond is present and $q=1-p$. Σl_j is the total number of bonds in the network in configuration $\{l_j\}$. We recall that B_t is the maximum number of bonds. Because of the energetic term which biases the probability distribution toward non stressed configurations, the actual number of bonds present in the network is different from pB_t, except in the infinite temperature limit. We may rewrite the partition sum as

$$\Omega_t(p,\beta) = \left(\frac{e^{\lambda}}{1+e^{\lambda}} \right)^{B_t} \sum_{\{l_j\}} e^{-\lambda \Sigma l_j} e^{-\beta N_{red}(\{l_j\})}, \quad (22)$$

where

$$\lambda = \ln\left(\frac{1-p}{p} \right). \quad (23)$$

We define $\omega(p,\beta) = \ln \Omega_t(p,\beta)/N_t$. Generalizing the renormalization transformation of the previous section, it is possible to compute exactly $\omega(p,\beta)$. We consider one elementary cell and want to compute $\varphi(p,\beta)$, the probability that this elementary cell is renormalized as a bond. The calculation is the same as in Sec. IV except that we have to attribute a weight $e^{-n\beta}$ instead of 1 to configurations with n redundant bonds. For the elementary cell of our chief example, Fig. 2(1), we use once again Table I to obtain

$$\varphi(p,\beta) = \frac{\varphi_1(p,\beta)}{\varphi_1(p,\beta) + \varphi_0(p,\beta)}, \quad (24)$$

where φ_1 collects the contributions of the configurations where the end sites of the cell are rigidly connected and φ_0 collects the contributions of the configurations where the end sites of the cell are not rigidly connected. Division by $\varphi_1 + \varphi_0$ is for normalization. We have

$$\varphi_1(p,\beta) = p^9 e^{-2\beta} + 9p^8 q e^{-\beta} + 30p^7 q^2 + 12p^6 q^3 + 3p^5 q^4,$$

$$\varphi_0(p,\beta) = 6p^7 q^2 e^{-\beta} + 2p^6 q^3 e^{-\beta} + 70p^6 q^3 + 123p^5 q^4 + 126p^4 q^5 + 84p^3 q^6 + 36p^2 q^7 + 9pq^8 + q^9. \quad (25)$$

Some curves $\varphi(p,\beta)$ are drawn for various values of β on Fig. 5. We also define

$$c(p,\beta) = \varphi_1(p,\beta) + \varphi_0(p,\beta). \quad (26)$$

Then, following the same reasoning as above, we derive the recursion relation:

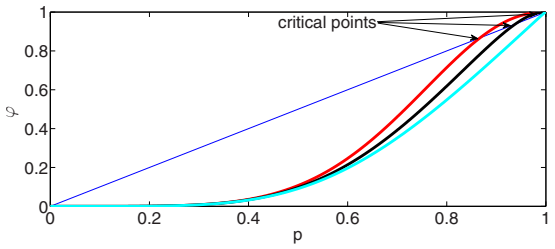

FIG. 5. (Color online) Examples of functions $\varphi(p,\beta)$, as a function of p; from left to right, $\beta=0,1,5$ (thick lines, respectively red, black, and light blue curves). The intersection with the $y=p$ straight line (blue thin line) is the critical point. A low temperature shifts the critical point toward high p values.

$$\Omega_t(p,\beta) = c(p,\beta)^{B_{t-1}}\Omega_{t-1}[\varphi(p,\beta),\beta]. \tag{27}$$

Taking the logarithm,

$$N_t\omega(p,\beta) = B_{t-1}\ \ln\ c(p,\beta) + N_{t-1}\omega[\varphi(p,\beta),\beta]. \tag{28}$$

Recalling that $N_t \simeq 3\times 9^t/8$ and $B_t=9^t$, we have

$$\omega(p,\beta) = \frac{8}{27}\ln\ c(p,\beta) + \frac{1}{9}\omega[\varphi(p,\beta),\beta]. \tag{29}$$

This yields the following expression for ω:

$$\omega(p,\beta) = \sum_{k=0}^{\infty}\frac{1}{9^k}\frac{8}{27}\ln\ c[\varphi^{(k)}(p,\beta)]. \tag{30}$$

As above, $\varphi^{(k)}$ is the kth iterate of the function φ. We note that the recursion relation for p depends parametrically on β and that the temperature is not renormalized in the process. This implies that there exists a line of critical points, and that the critical exponents continuously depend on β along this line. From Eqs. (22) and (23), we obtain an expression for $x(p,\beta)$

$$x(p,\beta) = \frac{8p}{3} + p(1-p)\frac{\partial\omega}{\partial p}. \tag{31}$$

We would like to study our model at fixed x; the previous formula tells us how to choose p to do so, providing the bridge between canonical and grand canonical ensembles. Figure 6 shows various $x(p)$ curves for different values of β. From Fig. 5, we can see that $p^*(\beta)$ tends to 1 for large β as we could have anticipated. However, the critical connectivity $x^*(\beta)$ does not tend to 8/3, see Fig. 6. A crucial observable is

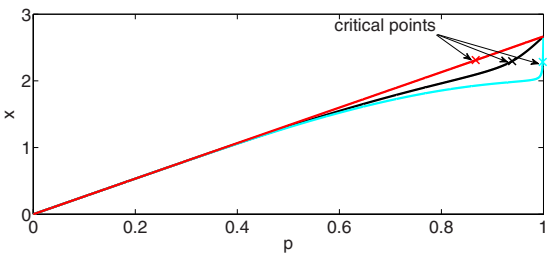

FIG. 6. (Color online) The mean connectivity of the network x as a function of p. From left to right, $\beta=0,1,5$ (respectively, red, black, and light blue curves). The critical points are also indicated.

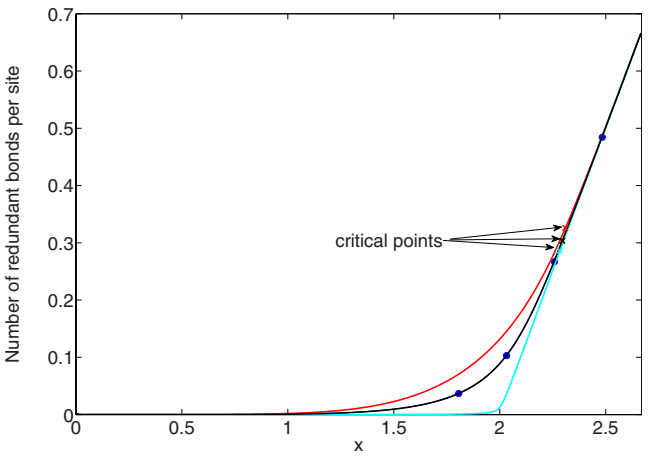

FIG. 7. (Color online) The number of redundant per site is plotted as a function of the mean connectivity x for $\beta=0,1,5$ (from left to right, respectively, red, black, and light blue curves). The crosses indicate the critical points; the filled circles are results of Metropolis Monte Carlo simulations, for $\beta=1$, using the pebble game algorithm, on hierarchical graphs with $t=5$ (22 145 sites). They are in perfect agreement with the analytical results.

the energy per site that is the number of redundant bonds per site n_{red}; it is computed using the formula:

$$n_{red} = \frac{\partial\omega}{\partial\beta}. \tag{32}$$

$n_{red}(p,\beta)$ curves are shown on Fig. 7, together with results of Monte Carlo simulations.

B. Intermediate phase

From the exact solution of the model provided in the previous paragraph, it is clear that the introduction of an energy and a finite temperature does not induce any qualitative change in the phase diagram: as a function of the connectivity, there are only two phases, floppy and rigid, separated by a phase transition at a critical connectivity $x^*(\beta)$. Thus, our first conclusion is that in this model, the intermediate phase does not have a real thermodynamical meaning. It is an important difference with the case of the random networks [24,25]. This result seems related to the strength of the percolation transition, which is first order in random networks and very weak on the hierarchical lattices introduced in this paper.

However, looking at the curves on Fig. 7, it is possible at low temperatures to distinguish three regions for low enough temperatures. At low connectivity $x<2$, there is essentially no redundant bond and thus no stress in the network; for $2<x<x^*(\beta)$, there is some stress in the network, but it does not percolate; finally, for $x>x^*(\beta)$, the stress percolates in the network. The boundary between the two first regions is not a thermodynamical transition; rather, it is a crossover which becomes sharper as the temperature decreases. In this crossover region, isostatic local structures are favored, and the effect of network self-organization is the strongest. To illustrate these points, we have plotted on Fig. 8 the fraction

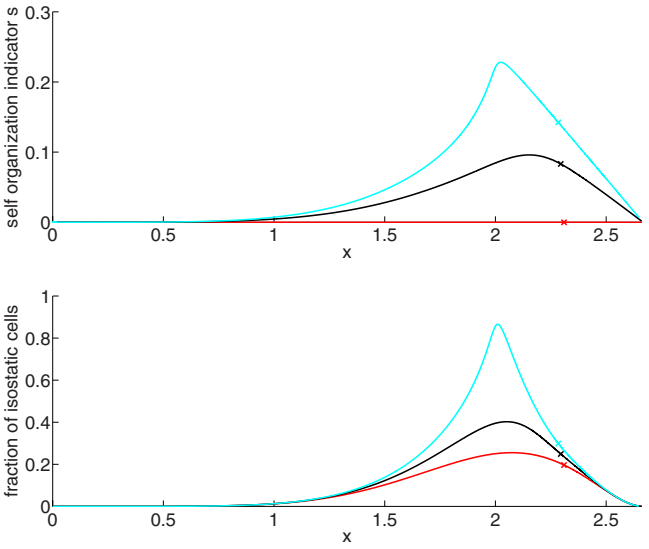

FIG. 8. (Color online) Top panel: the self organization indicator $s=(p-3x/8)/p$ as a function of the mean connectivity x. Bottom panel: fraction of isostatic elementary cells as a function of the mean connectivity. In both panels, $\beta=0,1,5$ from bottom to top (respectively, red, black, and light blue curves), and the crosses indicate the critical points. Note that s is identically 0 when $\beta=0$.

of isostatic elementary cells (with exactly seven bonds). To define an indicator for self-organization, we note that without network adaptivity (or equivalently at infinite temperature), the mean connectivity x is directly proportional to the parameter p and given by $x=8p/3$; we may then define a self-organization indicator as $s=(p-3x/8)/p$. s is plotted on Fig. 8 and peaks in the crossover region, just as the fraction of elementary cells. The lower the temperature, the sharper the peaks get.

Finally, we stress that we find a percolation transition at a critical density $x_c \simeq 2.3$, larger than the Maxwell threshold $x_{\mathrm{Max}}=2$. This contrasts with rigidity models on random graphs, for which the critical density is usually lower than x_{Max}.

VI. CONCLUSION

Our first result is the construction of solvable models for rigidity percolation, beyond trees, and random networks. These models display a critical point at the rigidity percolation threshold, and the critical exponent for the number of redundant bonds (which corresponds to the free energy) can be computed exactly. It would be interesting to compute also the exponent associated with the biggest rigid cluster in the network. In any case, it is known that these exponents, computed on such hierarchical networks, cannot be taken as reliable estimates for the exponents associated to regular lattices. However, these exponents may converge to the correct ones when one considers larger and larger cells for the hierarchical networks [34]. One may then think of a large cell Monte Carlo renormalization procedure to obtain an estimation of the critical exponents for 2D generic rigidity percolation. Some words of caution are in order: it is not clear how to extend to large sizes the hierarchical networks considered in this paper nor if they may be a good approximation of a regular lattice even for large cell sizes. It may be necessary to introduce other types of hierarchical lattices.

Our second result concerns the effect of self organization on rigidity percolation for these hierarchical models. We define and solve exactly a model where the network may adapt its structure to avoid stress at an entropic cost. At variance with what happens for random networks, the possibility of self-organization does not introduce a qualitative change in the phase diagram. In particular, there is no true thermodynamic intermediate phase. It may still be possible to define an intermediate region, where the network is close to be isostatic, and the stress does not percolate although it is present locally. It would be interesting to compare the properties of this intermediate region with the picture of the intermediate phase drawn from a size increasing cluster approximation [22]. From the modeling point of view, we note that a scenario where sharp phase transitions are replaced by smoother crossovers may still be compatible with the experiments on network glasses.

All our analysis relies on the combinatorial description of 2D generic rigidity. It should be possible to study similar hierarchical models of 3D rigidity with bond bending constraints using the associated combinatorial description [35]. It is not clear however how to generalize the technique to 3D networks with central forces only as there is no simple combinatorial description in that case (see [36] for a recent discussion).

ACKNOWLEDGMENTS

The author warmly thanks M. Chubynsky for making available to him his implementation of the pebble game algorithm and acknowledges useful discussions with S. Redner.

[1] J. C. Phillips, J. Non-Cryst. Solids **34**, 153 (1979).
[2] M. F. Thorpe, J. Non-Cryst. Solids **57**, 355 (1983).
[3] M. Latva-Kokko and J. Timonen, Phys. Rev. E **64**, 066117 (2001).
[4] D. A. Head, A. J. Levine, and F. C. MacKintosh, Phys. Rev. Lett. **91**, 108102 (2003).
[5] D. J. Jacobs and B. Hendrickson, J. Comput. Phys. **137**, 346 (1997).
[6] D. J. Jacobs and M. F. Thorpe, Phys. Rev. Lett. **75**, 4051 (1995).
[7] C. Moukarzel and P. M. Duxbury, Phys. Rev. Lett. **75**, 4055 (1995).
[8] G. Laman, J. Eng. Math. **4**, 331 (1970).
[9] D. J. Jacobs and M. F. Thorpe, Phys. Rev. E **53**, 3682 (1996).

[10] P. M. Duxbury, D. J. Jacobs, M. F. Thorpe, and C. Moukarzel, Phys. Rev. E **59**, 2084 (1999).
[11] S. P. Obukhov, Phys. Rev. Lett. **74**, 4472 (1995).
[12] C. Moukarzel, P. M. Duxbury, and P. L. Leath, Phys. Rev. E **55**, 5800 (1997).
[13] M. F. Thorpe, D. J. Jacobs, M. V. Chubinsky, and A. J. Rader, in *Rigidity Theory and Applications*, edited by M. F. Thorpe and P. M. Duxbury (Kluwer Academic/Plenum, New York, 1999).
[14] M. V. Chubinsky, Ph.D thesis, Michigan State University, 2003.
[15] J. Barré, A. Bishop, T. Lookman, and A. Saxena, J. Stat. Phys. **118**, 1057 (2005).
[16] S. Feng and M. Sahimi, Phys. Rev. B **31**, 1671 (1985).
[17] M. A. Knackstedt and M. Sahimi, J. Stat. Phys. **69**, 887 (1992).
[18] M. F. Thorpe, D. J. Jacobs, M. V. Chubinsky, and J. C. Phillips, J. Non-Cryst. Solids **266-269**, 859 (2000).
[19] D. Selvanathan, W. J. Bresser, and P. Boolchand, Phys. Rev. B **61**, 15061 (2000).
[20] Y. Wang, P. Boolchand, and M. Micoulaut, Europhys. Lett. **52**, 633 (2000).
[21] P. Boolchand, X. Feng, and W. J. Bresser, J. Non-Cryst. Solids **293-295**, 348 (2001).
[22] M. Micoulaut, Europhys. Lett. **58**, 830 (2002).
[23] M. Micoulaut and J. C. Phillips, Phys. Rev. B **67**, 104204 (2003).
[24] J. Barré, A. R. Bishop, T. Lookman, and A. Saxena, Phys. Rev. Lett. **94**, 208701 (2005).
[25] O. Rivoire and J. Barré, Phys. Rev. Lett. **97**, 148701 (2006).
[26] M. V. Chubynsky, M.-A. Brière, and N. Mousseau, Phys. Rev. E **74**, 016116 (2006).
[27] M.-A. Brière, M. V. Chubynsky, and N. Mousseau, Phys. Rev. E **75**, 056108 (2007).
[28] A. Sartbaeva, S. A. Wells, A. Huerta, and M. F. Thorpe, Phys. Rev. B **75**, 224204 (2007).
[29] M. Micoulaut and J. C. Phillips, J. Non-Cryst. Solids **353**, 1732 (2007).
[30] M. Chubynsky, in *Ridigity and Intermediate Phases in Nanomaterials*, edited by M. Micoulaut and M. Popescu (INOE Publishing House, Bucarest, 2009).
[31] A. N. Berker and S. Ostlund, J. Phys. C **12**, 4961 (1979).
[32] M. Kaufman and R. B. Griffiths, Phys. Rev. B **24**, 496 (1981).
[33] R. B. Griffiths and M. Kaufman, Phys. Rev. B **26**, 5022 (1982).
[34] P. J. Reynolds, H. E. Stanley, and W. Klein, Phys. Rev. B **21**, 1223 (1980).
[35] D. J. Jacobs, J. Phys. A **31**, 6653 (1998).
[36] M. V. Chubynsky and M. F. Thorpe, Phys. Rev. E **76**, 041135 (2007).
[37] An embedding of a graph in $\mathbb{R}^2$ is said to be generic if sites and bonds do not present any "special" property, such as two parallel bonds or three aligned sites. For a clear and rigorous presentation of generic 2D rigidity, see for instance [5].